# Dynamic control of hydrogel crosslinking via sortase-mediated reversible transpeptidation

Matthew R. Arkenberg, Dustin M. Moore, and Chien-Chi Lin*

*Department of Biomedical Engineering, Purdue School of Engineering & Technology, Indiana University-Purdue University Indianapolis, Indianapolis, IN 46202, USA*

*To whom correspondence should be sent:

Chien-Chi Lin, PhD.
Associate Professor
Department of Biomedical Engineering
Purdue School of Engineering & Technology
Indiana University-Purdue University Indianapolis
Indianapolis, IN 46202
Phone: (317) 274-0760
Email: lincc@iupui.edu

**Abstract**

Cell-laden hydrogels whose crosslinking density can be dynamically and reversibly tuned are highly sought-after for studying pathophysiological cellular fate processes, including embryogenesis, fibrosis, and tumorigenesis. Special efforts have focused on controlling network crosslinking in poly(ethylene glycol) (PEG) based hydrogels to evaluate the impact of matrix mechanics on cell proliferation, morphogenesis, and differentiation. In this study, we sought to design dynamic PEG-peptide hydrogels that permit cyclic/reversible stiffening and softening. This was achieved by utilizing reversible enzymatic reactions that afford specificity, biorthogonality, and predictable reaction kinetics. To that end, we prepared PEG-peptide conjugates to enable sortase A (SrtA) induced tunable hydrogel crosslinking independent of macromer contents. Uniquely, these hydrogels can be completely degraded by the same enzymatic reactions and the degradation rate can be tuned from hours to days. We further synthesized SrtA-sensitive peptide linker (i.e., KCLPRTGCK) for crosslinking with 8-arm PEG-norbornene (PEG8NB) via thiol-norbornene photocrosslinking. These hydrogels afford diverse softening paradigms through control of network structures during crosslinking or by adjusting enzymatic parameters during on-demand softening. Importantly, user-controlled hydrogel softening promoted spreading of human mesenchymal stem cells (hMSCs) in 3D. Finally, we designed a bis-cysteine-bearing linear peptide flanked with SrtA substrates at the peptide's N- and C-termini (i.e., $NH_2$-GGGCKGGGKCLPRTG-$CONH_2$) to enable cyclic/reversible hydrogel stiffening/softening. We show that matrix stiffening and softening play a crucial role in growth and chemoresistance in pancreatic cancer cells. These results represent the first dynamic hydrogel platform that affords cyclic gel stiffening/softening based on reversible enzymatic reactions. More importantly, the chemical motifs that affords such reversible crosslinking were built-in on the linear peptide crosslinker without any post-synthesis modification.

**Keywords**: Sortase A; dynamic hydrogels; extracellular matrix; cancer; tissue stiffening

## 1. Introduction

Stiffening and softening of extracellular matrix (ECM) contribute to many biological processes including cancer progression, stem cell differentiation, and tissue fibrosis [1-3]. Specifically, mechanical properties of ECM affect changes in cellular morphologies [4, 5], protein expression and secretion [6], and stem cell differentiation potentials [7, 8]. For example, matrix stiffening has been shown to promote aggressive phenotypes, epithelial-to-mesenchymal transition (EMT), and chemo-resistance in pancreatic ductal adenocarcinoma (PDAC) [1, 9]. On the molecular level, prior studies have established a causal link between matrix stiffness and nuclear localization of yes-associated protein (YAP). In particular, Rice and colleagues reported that increasing matrix stiffness (~1 kPa to ~4 kPa) lead to an increase in YAP nuclear localization in three different pancreatic cancer cell lines [9]. Nguyen and colleagues identified higher matrix moduli (~3 kPa) promoted metastatic potential of PDAC cell lines [10]. On the other hand, matrix softening was shown to reduce sensitivity of myeloid leukemia subtypes to chemotherapeutics [11]. ECM biophysical stimuli also affect morphology and differentiation potentials of human mesenchymal stem cells (hMSCs). Discher and colleagues demonstrated that culturing hMSCs on soft (0.1-1kPa) substrates yielded cellular morphology akin to neurogenic lineage, whereas stiffer substrate (25-40 kPa) promoted osteogenic differentiation [12].

Cell fate processes have been increasingly studied using cell-laden three-dimensional (3D) hydrogels. However, hydrogels with static mechanical properties may not fully recapitulate the dynamic nature of tissue mechanics [13-20] and few 3D culture materials permit user-initiated control over matrix physiochemical properties [21-23]. Recent efforts on ‘dynamic’ hydrogels have allowed researchers to control matrix stiffening and/or softening patterns that mimic the ever-changing ECM microenvironment. ‘Stiffening’ hydrogels are often designed to permit secondary crosslinking upon exposure to external stimuli such as light, temperature, pH,

or enzymes. On the other hand, hydrolytic [24-26] or enzymatic cleavage [27, 28] are typically utilized to soften matrices without user intervention. User-controlled matrix softening can be achieved through the addition of photoresponsive linkers [29]. For example, Anseth and colleagues developed elegant photodegradable hydrogels that permit the investigation of local matrix softening on cell behaviors [29]. Rosales et al. [14, 19], Zheng et al. [15], and Lee et al. [18] fabricated hydrogels with photoswitchable azobenzene moieties that afford reversible control of stiffness. Reversible tuning of matrix stiffness is achieved upon irradiation with the appropriate wavelength of light. In another example, controlling diol and boronic acid reactivity through azobenzene cis-trans transition was implemented to dynamically stiffen hydrogels [16]. Our group has also utilized supramolecular host-guest interactions to reversibly stiffen and soften hydrogels [17].

The above examples highlight the importance of creating a hydrogel network with reversible stiffening/softening capability. To this end, enzymatic reactions can afford substrate specificity and mild/predictable reaction kinetics [23, 30-36]. Our lab has previously utilized mushroom tyrosinase (MT) to dynamically stiffen hydrogels containing either tyrosine residues [23, 36] or 4-hydroxyphenyl acetic acid (HPA) [35]. We have also reported the design of PEG-peptide hydrogels that were sensitive to both MT and sortase A (SrtA). The hydrogels were susceptible to orthogonal and enzymatic control of crosslinking and on-demand stiffening [36]. While MT-mediated tyrosine dimerization affords efficient stiffening regimes, this enzymatic reaction is limited by the availability of dissolved molecular oxygen, the irreversibility of the di-tyrosine products, and unexpected oxidation of tyrosine-rich proteins. These disadvantages could be circumvented by using SrtA, a cysteine transpeptidase highly useful in site-specific protein labeling [37-41], peptide cyclization [42-46], and antibody modification [47-51]. Mechanistically, SrtA cleaves the amide bond between threonine and glycine residues of the LPXTG (where X is any amino acid except proline) sequence, resulting in a thiol-acyl

intermediate that is subsequently resolved by an oligoglycine substrate ($G_n$). The end product of this enzymatic reaction is a new peptide sequence LPXT($G_n$) (**Fig. 1A**) that itself serves as a substrate for further SrtA transpeptidation. Of note, this reaction is also susceptible to hydrolysis, resulting in the formation of an unreactive pendant LPRT-OH [52]. Nonetheless, this biorthogonal enzymatic reaction can be utilized to crosslink, degrade, and modify hydrogels by incorporating the peptide substrates into the super structure of the hydrogels. Specifically, the LPXTG and $G_n$ peptides can be tethered to macromers using either Michael-type addition [53, 54] or thiol-norbornene click chemistry [36]. Upon addition of SrtA, the peptides are ligated to create new crosslinks. Broguire *et al.* recently reported the use of SrtA to crosslink hyaluronic acid-based hydrogels for tissue engineering applications [53]. In another example, Griffith and colleagues incorporated SrtA-labile LPXTG substrate as part of the linkers in hydrogels formed by either Michael-type or thiol-norbornene chemistry [54]. Addition of SrtA and soluble glycine led to breakage of the LPETG peptide, eventually resulted in degradation of the hydrogels.

In this work, we attempt to expand the utility of SrtA-mediated transpeptidation to: (1) control hydrogel crosslinking and degradation; (2) permit controllable degrees of hydrogel softening; and (3) enable reversible stiffening and softening of PEG-peptide hydrogels. We used a hepta-mutant variant of SrtA for its increased catalytic activity and calcium-independency [39, 55, 56]. We designed simple linear peptide linkers containing SrtA-specific sequences to afford rapid and controllable crosslinking of PEG-peptide hydrogels. These gels can be dissolved/degraded within hours to days. We also used a SrtA-sensitive peptide crosslinker to afford controllable softening and the matrix was leveraged to control spreading of hMSCs in 3D. Finally, we designed a linear bis-cysteine peptide crosslinker whose N- and C-terminus was flanked with the two SrtA substrates to demonstrate cyclic/reversible hydrogel stiffening and softening. Most importantly, this dynamic cell culture platform was exploited for studying stiffness-dependent growth and chemo-resistance in pancreatic cancer cells (PCCs).

## 2. Materials & Methods

### 2.1 Materials

Eight-arm PEG-OH (20 kDa) was acquired from JenKem Technology, USA. 5-Norbornene-2-carboxylic acid, N,N-dicyclohexylcarbodiimide (DCC), 4-(dimethylamino)pyridine (DMAP), dimethyl phenylphosphonite, 2,4,6-trimethylbenzoyl chloride, 2-butanone, lithium bromide, diethyl ether, and Isopropyl-D-1 thogalactopyranoside (IPTG) were obtained from Sigma-Aldrich. Fmoc-protected amino acids N,N,N,N -tetramethyl-O-(1H-benzotriazol-1-yl)uranium hexafluorphosphate (HBTU), and hydroxybenzotriazole (HOBt) were purchased from Anaspec. BL21 Escherichia coli (E. coli) was purchased from New England Biolabs. Kanamycin sulfate was obtained from IBI Scientific. Lysogeny broth, Lennox formulation, agar and broth were obtained from DOT Scientific. Gemcitabine was obtained from TSZ CHEM. Mammalian cell Live/Dead staining kit was obtained from Life Technologies Corp. All other chemicals were obtained from Fisher Scientific unless otherwise noted.

### 2.2 Macromer and peptide synthesis

Eight arm PEG-norbornene (PEG8NB, ~95% substitution) and photoinitiator lithium aryl phosphinate (LAP) were synthesized as described previously [36, 57]. Peptides were synthesized in an automated microwave-assisted peptide synthesizer (Liberty 1, CEM). Crude peptides bound to resin were reacted with a solution containing 95% trifluoroacetic acid (TFA), 2.5% $ddH_2O$, 2.5% triisopropylsilane (TIS), and 5% (w/v) phenol for 3 hours at room temperature for cleavage. Immediately following cleavage, the peptides were precipitated in cold ethyl ether. Dried, crude peptides were purified using High-Performance Liquid Chromatography (HPLC, Flexar System, Perkin Elmer). Purified peptides were lyophilized and their masses confirmed via mass spectrometry (Agilent Technologies). All peptides were stored at -20$^{o}$C prior to use.

### 2.3 Heptamutant SrtA expression and purification

Heptamutant SrtA (P94R, E105K, E108Q, D160N, D165A, K190E, K196T) was expressed and purified as described previously [36, 58]. Competent BL21 *E. coli* were transformed with pet30b-7M SrtA plasmid (a gift from Hidde Ploegh. Addgene plasmid #51141) and grown on an LB-agar selection plate containing kanamycin (30 µg/mL). Individual colonies were inoculated in 10 mL of LB broth supplemented with kanamycin (30 µg/mL). After overnight shaking (220 rpm, 37 $^{o}$C), the cultures were diluted 100-fold in LB media supplemented with kanamycin and placed on an orbital shaker (220 rpm at 37 $^{o}$C), and the optical density at 600 nm ($OD_{600}$) was monitored. SrtA expression was induced at $OD_{600}$ = 0.4-0.6 by adding IPTG (400 µM) to the cultures and shaking for 3 hours at 37 $^{o}$C and 220 rpm. Following induction, the cell pellets were isolated by centrifugation (8000 rpm, 15 minutes) and stored at -80 $^{o}$C prior to lysis. Cell lysis was performed by suspending the pellets in lysis buffer (20 mM Tris, 50 mM NaCl, 0.2 mg/mL lysozyme, 1x Halt EDTA-free protease inhibitor cocktail, and DNase I). Following a 30-minute incubation at 4 $^{o}$C, the suspended pellets were subject to sonication (2 cycles of 3 minutes with 30% duty cycle, 20% amplitude followed by a 3-minute cool-down period). Lysates were clarified by centrifugation (10000 x g, 20 min, 4 $^{o}$C) and purified via His60 Ni Superflow resin and columns per manufacturer's protocol. Purified SrtA (~40 mg/L of culture) was concentrated with Ultra-15 Centrifugal Filter Units (3 kDa MWCO, Amicon) and desalted with Zeba Spin desalting columns (7 kDa MWCO, Thermo Fisher Scientific). The enzyme in PBS (pH = 7.4) was aliquoted, flash frozen, and stored at -80 $^{o}$C Stock concentrations of SrtA were obtained by Ellman's assay measuring the free sulfhydryl on SrtA. Typical concentrations of SrtA stock aliquots were ~4 mM.

**2.4 Sortase A-mediated hydrogel crosslinking and degradation**

PEG-peptide conjugates (i.e., PEG-GGGG and PEG-LPRTG) were prepared by reacting free norbornene groups of PEG8NB with cysteine-bearing peptides via thiol-norbornene photoclick chemistry. GGGGC or LPRTGC peptides were separately dissolved in PBS (pH =

7.4) prior to quantification of their concentrations with Ellman's assay. To a round bottom flask, PEG8NB, peptides (1.5-fold excess to norbornene moieties), and photoinitiator LAP (5 mM) were added. The conjugation of peptide to PEG8NB was initiated upon exposure to light (Omnicure s1000, 365 nm, 40 mW/cm$^2$) for 30 minutes. Additional LAP was added at 15 minutes to improve conjugation efficiency. The PEG-peptide conjugates were dialyzed against dd$H_2O$ for 2 days to remove residual peptides and LAP. Using TNBSA assay, we determined the amine group concentration of the PEG-GGGG conjugate (~2.66 mM/wt% of PEG-GGG). Note that the PEG-peptide conjugates can also be prepared by Michael-type reaction between cysteine-bearing peptides and multi-arm PEG-vinylsulfone or PEG-maleimide. It is also worth noting that the cysteine residue at the active site of SrtA is not reactive towards norbornene groups as the thiol-norbornene reaction only occurs under radical-mediated light exposure. The purified conjugates were lyophilized and stored at -20$^o$C prior to use.

To initiate gelation, PEG-peptide conjugates were mixed in the presence of SrtA and immediately injected between glass slides separated by 1 mm Teflon spacers. After 10 minutes of gelation, the hydrogels were transferred to a 24-well plate containing PBS. The hydrogels were washed three times with PBS (30 min per wash) to remove residual SrtA and incubated at 37$^o$C for 16 hours prior to degradation studies. After SrtA-mediated gelation, the initial masses ($W_o$) of the hydrogels were measured, followed by placing the hydrogels in buffer solution containing specified concentrations of: (1) SrtA with soluble glycinamide for transpeptidation-mediated degradation, or (2) SrtA alone for hydrolytic degradation. At specified time points, the hydrogels were removed from the degradation buffers, blotted dry, weighed ($W_t$), and returned to solution. This process was repeated until the hydrogels were fully degraded. For the hydrolytic degradation, fresh SrtA-containing buffer was exchanged after 24 hours of incubation. The results were presented as: Mass loss (%) = 100% × ($W_t$-$W_0$)/$W_0$.

**2.5 Thiol-norbornene photopolymerization of SrtA-responsive hydrogels**

For experiments related to tuning matrix stiffening and softening, hydrogels were fabricated by reacting PEG8NB and bis-cysteine containing peptides (e.g., KC-LPRTG-CK, KC-LPRTA-CK, or GGG-CKGGGKC-LPRTG) via thiol-norbornene photoclick chemistry. Briefly, PEG8NB and peptides were mixed at a stoichiometric ratio of thiol to norbornene along with photoinitiator LAP (1 mM). The precursor solution with pre-defined compositions was injected between two glass slides separated by 1 mm Teflon spacers, followed by exposure to 365 nm light (5 mW/cm$^2$) for 2 minutes. The obtained hydrogels were swollen for 16 hours in PBS prior to dynamic stiffening or softening.

**2.6 Sortase A-mediated hydrogel softening & stiffening**

Controlled softening of PEG-peptide hydrogels was achieved by incubating the swollen gels in buffer solution containing specified concentrations of SrtA and oligoglycine substrate (GGGGC, glycinamide, etc.). Storage moduli of the gels were measured before softening and at specified time points during, and after softening using oscillatory rheometry in strain sweep mode (8 mm parallel plate geometry, 0.1% to 5% strain at 1 Hz frequency).

Swollen hydrogels were incubated with solutions containing either SrtA or SrtA with soluble glycine to induce stiffening or softening, respectively. After each incubation step, SrtA or SrtA with soluble glycine buffers were replaced with phosphate-buffered saline solution (PBS, pH = 7.4) after incubation to remove residual SrtA. Storage moduli were measured prior to and after stiffening or softening. The gap sizes were reduced from 750 to 500 μm for stiffening and increased to 650 μm after softening due to observed volumetric shrinkage or swelling.

**2.7 Cell culture and encapsulation**

Human mesenchymal stem cells were maintained in low glucose Dulbecco's Modified Eagle's Medium (DMEM) supplemented with 10% fetal bovine serum (FBS), 1 ng/mL basic fibroblast growth factor (bFGF), and 1x-penicillin streptomycin. Briefly bFGF was supplemented

in the media at 1 ng/mL as the concentration has been shown to maintain viability and proliferation of hMSCs during in vitro culture [59]. Media was refreshed every 2-3 days. PDAC cell line COLO-357 were maintained in high glucose DMEM supplemented with 10% FBS and 1x-penicillin streptomycin. For encapsulation, hMSCs and COLO-357 cells were rinsed with Dulbecco's phosphate-buffered saline (DPBS), trypsinized, counted via hemocytometry, and resuspended at specified cell density in DPBS. The cells were mixed with sterile-filtered (0.2 µm) pre-polymer solutions containing PEG8NB, peptide crosslinkers (KCLPRTGCK, KCLPRTACK, or GGG-CKGGGKC-LPRTG), and LAP (1 mM). The solution was mixed and pipetted into a 1 mL syringe with cut-open tip. Cell-laden gels were cast upon exposure to 365 nm light (5 mW/cm$^2$) for 2 minutes and placed in a 24-well plate with fresh media. For the hMSC study, 3.5 wt% PEG-peptide gels were crosslinked with: (1) MMP-labile crosslinks (KCGPQG↑IWGQCK) for cell-mediated local degradation, (2) pendant CRGDS (1 mM) for cell adhesion, and (3) 'G' peptide linkage for SrtA-mediated softening ('A' peptide was used as control).

**2.8 Softening of hMSC-laden hydrogels**

Following encapsulation, hMSC-laden hydrogels were cultured in media for 7 days prior to SrtA-induced softening. Media was refreshed every 2-3 days. Softening was achieved through incubation of hydrogels in media containing 25 µM SrtA and 12 mM glycinamide for 4 hours on day 7 post-encapsulation. Gels were subsequently washed with fresh media for 4 hours to remove SrtA and glycinamide. Live/dead staining and confocal microscopy imaging were performed on day 1, 7, and 14 post-encapsulation to assess cell viability and morphology. At least three z-stacked images per gel (10 slices, 100 µm thick) were taken. F-actin and DAPI staining and confocal imaging were performed on day 14 post-encapsulation for assessing cytoskeletal structure and cell morphology. Circularity and average cell area values were measured using ImageJ software and the F-actin/DAPI stained confocal images. Circularity is

quantified as $4\pi(\frac{\text{Area}}{\text{Perimeter}^2})$ and the area was quantified using the "Analyze Particles" function in ImageJ.

### 2.9 Reversible stiffening of COLO-357-laden hydrogels and related assays

COLO-357-laden hydrogels (2.5 wt% PEG8NB) were incubated in media for 7 days prior to matrix stiffening. Static controls include soft (2.5 wt% PEG8NB) and stiff (3.5 wt% PEG8NB) hydrogels that were not responsive to SrtA treatment. To induce matrix stiffening, hydrogels were placed in media supplemented with 50 μM of SrtA and incubated for 4 hours. On day 14 post-encapsulation, the hydrogels were placed in media with 50 μM of SrtA and 15 mM of soluble glycine substrate to induce softening. Live/dead staining and confocal microscopy imaging were performed on day 1, 7, 14, and 21 to assess cell viability and spheroid morphology. The spheroid diameters were measured using Nikon NIS-element software.

For the gemcitabine treatment study, COLO-357 cells were allowed to grow into spheroids for 4 days prior to SrtA-induced stiffening (50 μM, 4 hours). On day 7, hydrogels were treated with SrtA (50 μM) and glycinamide (15 mM) to induce softening. On day 10, these 'softened' cell-laden hydrogels were treated with gemcitabine (1 μM) for 3 additional days prior to live/dead staining and imaging on day 13. Control groups include cell-laden hydrogels that only went through stiffening (i.e., Stiffened group), non-dynamic soft (i.e., Soft group. G' ~ 1 kPa), and non-dynamic stiff (i.e., Stiff group. G' ~ 3 kPa). Metabolic activity was assessed via AlamarBlue reagent before and after gemcitabine treatment. Viability and spheroid morphology were monitored via live/dead staining and confocal imaging as described above.

### 2.10 Statistical analysis

A two-way analysis of variance (ANOVA) with a Bonferroni *post-hoc* test to evaluate significance between experimental groups. For spheroid diameter experiments, two-way ANOVA was performed on the average diameter between three values from independent

experiments with three time points (i.e., day 7, day 14, and day 21). Single, double, and triple asterisks represent $p < 0.05$, 0.01, 0.001, respectively. All experiments were completed independently thrice. Quantitative results are presented as mean ± SEM.

## 3. Results

### 3.1 SrtA-mediated crosslinking of PEG-peptide hydrogels

In order to exploit SrtA-initiated transpeptidation (**Fig. 1A**) for crosslinking of PEG-peptide hydrogels, we conjugated PEG8NB macromers with cysteine-bearing SrtA substrates (i.e., $NH_2$-GGGGC-$NH_2$ and $NH_2$-CLPRTG-$NH_2$) via thiol-norbornene photoclick chemistry. Notably, the substitution of the peptide conjugate was approximately 70% as measured by TNBSA assay. In addition to the inherent limitation on peptide conjugation efficiency, it is also possible that some peptides were 'damaged' during the conjugation process. However, we showed that the resulting PEG-peptide conjugates were still functional and could be used to crosslink hydrogels using SrtA-initiated transpeptidation (**Fig. 1B**). At a fixed total PEG-peptide macromer content (6 wt%), gelation speed could be independently tuned from 10 minutes with 300 μM SrtA to 90 minutes with 50 μM SrtA (**Fig. 1C**).

### 3.2 SrtA-mediated hydrolytic degradation of SrtA-crosslinked PEG-peptide hydrogels

The reversibility of SrtA-mediated transpeptidation affords control not only in hydrogel crosslinking, but also in temporal degradation of PEG-peptide hydrogels. Specifically, hydrogels were degraded on-demand through addition of SrtA and soluble glycine substrates (e.g., glycinamide), which induce transpeptidation-based degradation (**Fig. 1A**). As concentrations of SrtA or glycinamide increased, gel degradation occurred significantly faster (**Figs. 2A and 2B**), as supported by the initial swelling (i.e., negative loss of mass) and then rapid mass loss of the gels. Complete degradation was achieved in approximately 5, 7, and 9 hours using 50, 25, and 10 μM of SrtA, respectively. At a fixed SrtA concentration (e.g., 25 μM), hydrogels treated with

16 or 48 mM of glycinamide (i.e., 1- and 3-fold to crosslinker concentration in hydrogels) degraded completely in 7 or 5 hours, respectively.

Incubation of hydrogels with SrtA alone permits slow hydrolytic degradation as water can react with the thioacyl intermediate to yield LPRT-OH (**Fig. 1A**) [52]. Compared with transpeptidation-mediated degradation, hydrolytic degradation occurs more slowly and has a nearly linear mass loss profiles (**Fig. 2C**). The hydrogels degraded in approximately 50 to 58 hours when using only 50 to 25 μM of SrtA (i.e., without glycinamide), respectively.

### 3.3 SrtA-mediated softening of thiol-norbornene PEG-peptide hydrogels

SrtA-initiated transpeptidation provides a high degree of control in crosslinking PEG-peptide conjugates into hydrogels. However, it is challenging to use this enzymatic reaction and hydrogel design to achieve controlled gel softening owing to the erosion of gel surface and mass loss upon encountering the enzyme. We hypothesized that a different PEG-peptide hydrogel architecture could prevent gel mass loss while permitting SrtA-mediated on-demand softening. To achieve this, we synthesized bis-cysteine peptides sensitive (KCLPRTGCK, “G” peptide) or insensitive (KCLPRTACK, “A” peptide) to SrtA-mediated transpeptidation. Cysteine residues were added to afford thiol-norbornene photo-click gelation between macromer PEG8NB with “G” and/or “A” peptides, whereas lysine residues were added to improve the solubility of the peptides. Upon incubation in a solution containing SrtA and an oligoglycine substrate, only SrtA-sensitive linkages (i.e., G peptide) underwent cleavage (**Fig. 3A**). Varying the concentrations of A and G crosslinkers within 3 wt% PEG8NB-peptide hydrogels resulted in tunable degrees of SrtA-induced gel softening (**Fig. 3B**). Specifically, A:G ratios of 100%:0%, 75%:25%, and 50%:50% respectively yielded 0-, 0.5-, and 0.75-fold moduli decrease compared with the initial modulus ($G'_o$). Next, we investigated the role of SrtA concentration on softening time (3 wt% PEG, A:G ratio = 50%:50%). Above 25 μM SrtA, there was no notable difference in softening time, but hydrogels incubated with only 10 μM SrtA were degraded in a slower rate

(**Fig. 3C**). Furthermore, hydrogels formed with 2.5, 3, or 3.5 wt% of PEG showed increasing initial moduli (~0.75, ~2.5 or ~3 kPa, respectively), which were softened upon SrtA treatment to 0.15, 0.75, or 1 kPa, respectively (**Fig. 3D**). In addition, hydrogels incubated in SrtA/oligoglycine substrate solution for 0.5, 2.5, and 4 hours softened to approximately 0.75, 0.5, and 0.2-fold of the initial modulus (**Fig. 3E**).

While hydrogels crosslinked with SrtA-sensitive peptide (i.e., LPRTG) permitted controlled softening, attempts to re-stiffen these softened gels yielded disappointing results. Specifically, the hydrogels could only be re-stiffened to about 20% of the original gel moduli (data not shown). This was likely due to the difficulty for the infused SrtA to 'reach' the 'broken' peptides simultaneously in a highly swollen hydrogel.

### 3.4 SrtA-mediated softening of hMSC-laden PEG-peptide hydrogels

The SrtA-induced softening hydrogels were used as a cell culture platform to evaluate the effect of temporal matrix softening on hMSCs spreading. In this study, hMSCs were encapsulated in hydrogels formed by 3.5 wt% PEG8NB with MMP-labile crosslinks (KCGPQG↑IWGQCK, for cell-mediated local degradation) and 'G' peptide linkage for SrtA-mediated softening ('A' peptide was used as control). Note that all cell-laden hydrogels also contained 1 mM CRGDS for promoting cell adhesion. Furthermore, peptide crosslinkers were mixed at 40% SrtA-responsive 'G' peptide (or SrtA insensitive 'A' peptide) and 60% MMP-sensitive peptide linker. Live/dead and F-actin/DAPI staining results showed that cells in both groups displayed mostly non-spreading morphology prior to SrtA-induced softening on day 7 (**Fig. 4A**). Note that a higher initial gel stiffness ($G'_0$ ~ 4 kPa) was used to demonstrate the effect of SrtA-mediated on-demand gel softening on cell fate processes. The high initial gel stiffness may be the reason causing noticeable number of dead cells on Day 1. By day 14, cells within the on-demand softened hydrogels adopted long and thin protrusions compared with cells encapsulated within statically stiff hydrogels. Semi-quantitative analysis of cell spreading

revealed a significant reduction in circularity (**Fig. 4B**) and increase in cell area (**Fig. 4C**) in cells experienced on-demand softening.

### 3.5 Reversible stiffening of PEG-peptide hydrogels

Owing to its unique reversibility in peptide conjugation, we hypothesized that SrtA can be used to create hydrogels with dynamically and reversibly tunable stiffness. We designed a linear peptide flanked with the two SrtA substrates (GGG-CGGGC-LPRTG) for crosslinking into hydrogels via thiol-norbornene photopolymerization. The N-terminal GGG and C-terminal LPRTG sequences became pendant motifs permitting SrtA-mediated secondary crosslinking and degradation, thus leading to cyclic/reversible hydrogel stiffening and softening (**Fig. 5A**). To optimize SrtA-mediated matrix stiffening, PEG-peptide hydrogels (2.5 wt%) were incubated with varying time and concentrations of SrtA. A 1.75- to 2.5-fold increase in gel modulus ($G'_0$ = 1 kPa) were observed upon 3 hours of incubation with 25 μM of SrtA (**Fig. 5B**). Furthermore, 2- to 4-fold increases in moduli were observed when 10 to 50 μM of SrtA were added for 4 hours (**Fig. 5C**).

The stiffened hydrogels could be further softened by incubating the hydrogels with SrtA alone or with SrtA and soluble glycine substrate. As shown in **Figure 5D,** moduli of the stiffened gels ($G'_{stiff}$ ~3 kPa) were decreased 0.8 to 0.5-fold with increasing concentrations of glycinamide, where maximum softening was achieved with 15 mM of soluble glycinamide and 25 μM of SrtA. SrtA-mediated hydrolytic degradation could also be utilized to soften hydrogels at a slower rate (**Fig. 5E**). For example, hydrogels incubated with SrtA alone (25 μM) were softened to approximately 0.4-fold of the initial gel modulus. Finally, multiple cycles of reversible gel stiffening/softening could be achieved by incubating hydrogels alternatively with SrtA (for stiffening) and SrtA and soluble glycinamide (for softening) (**Figure 6**).

### 3.6 Effect of stiffening and softening on COLO-357 viability and spheroid formation

To demonstrate the feasibility of using SrtA-mediated reversible stiffening hydrogels as a platform for investigating cell fate processes, COLO-357 cells were encapsulated in SrtA-sensitive hydrogels and exposed to stiffening and softening conditions. Cell-laden soft (2.5 wt% PEG8NB, G' ~ 1 kPa) and stiff (3.5 wt% PEG8NB, G' ~ 3 kPa) hydrogels were utilized as controls (i.e., without dynamic stiffening). Dynamically-stiffened PEG-peptide hydrogels (2.5 wt% PEG8NB) formed with pendant SrtA substrates (i.e., GGG-CGGGC-LPRTG) were stiffened on day 7 and softened on day 14 (**Fig. 7A**). Per the confocal images, both the initial thiol-norbornene gel crosslinking and SrtA-mediated stiffening/softening were cytocompatible as indicated by the high cell viability (**Fig. 7B**). We quantified diameters of the cell spheroids and found that when cultured in 'statically soft' hydrogels, the spheroid sizes grew steadily from ~40 µm to ~51 µm over 21 days (**Fig. 7C, Table 1**). On the other hand, the growth was significantly hindered in cells maintained in 'statically stiff' hydrogels (**Fig. 7D, Table 1**). In the dynamic hydrogel group (i.e., Soft-Stiff-Soft), the growth of spheroids was initially delayed following stiffening (from D7 to D14). Subsequent softening of the hydrogels allowed the cell spheroids to grow again (**Fig. 7E, Table 1**). The patterns of spheroid size changes in the 'Soft-Stiff-Soft' hydrogels demonstrate the effect of dynamic matrix stiffening/softening on PCC growth.

**Table 1.** Summary of average spheroid diameters in Figure 7.

| Day | Soft (µm) | Soft-Stiff-Soft (µm) | Stiff (µm) |
|---|---|---|---|
| **7** | $40.08 \pm 0.75^{ab}$ | $40.76 \pm 0.76^{c}$ | $34.07 \pm 0.84$ |
| **14** | $48.45 \pm 3.30^{a}$ | $39.60 \pm 1.84^{d}$ | $33.85 \pm 0.35$ |
| **21** | $51.36 \pm 2.77^{b}$ | $47.89 \pm 1.49^{cd}$ | $32.41 \pm 0.51$ |

*Note: Superscripts "a" and "d" represent $p < 0.01$. Subscripts "b" and "c" denote $p < 0.001$ and $p < 0.05$, respectively.*

### 3.7 Effect of matrix stiffening on the chemoresistance of encapsulated COLO-357 cells

**Figure 8** shows the effect of cyclic matrix stiffening/softening on growth of COLO-357 cells under gemcitabine treatment (**Fig. 8A**). Live/dead staining results show that gemcitabine treatment only caused significant cell death in non-dynamic soft hydrogels (**Fig. 8B**) but not in

non-dynamic stiff hydrogels (**Fig. 8C**). In the dynamic 'stiffened' group, which mimics the effect of drug treatment in a stiffened stromal tissue, gemcitabine treatment caused limited amount of cell death (**Fig. 8D**). Finally, in the dynamic 'softened' group, which mimics the effect of softening a stiffened stromal tissue, gemcitabine treatment only led to some cell death (**Fig. 8E**) when compared with that in the non-dynamic soft hydrogels (**Fig. 8B**). AlamarBlue assay results mirrored the results in the live/dead staining images where only cells encapsulated in soft or softened hydrogels exhibited reduced metabolic activity upon gemcitabine addition, whereas cells in the stiffen or stiffened hydrogels were non-responsive to gemcitabine treatment (**Fig. 8F**).

## 4. Discussion

Investigating the role of biophysical and biochemical cues on cell fate processes is highly challenging owing to the complex, heterogeneous, and dynamically changing nature of the ECM. Commercially available 3D culture platforms such as Matrigel® afford convenience, but lack well-defined or tunable properties. Additionally, static 3D hydrogels do not provide spatiotemporal control of matrix properties critical for guiding cell fate processes. Accumulating evidence suggests that matrix stiffness plays an integral role in cell mechanobiology. Therefore, designing 'four-dimensional' cell culture platforms are necessary for studying these phenomena. Our lab has utilized enzymatic strategies to dynamically control hydrogel crosslinking [23, 35, 36]. We have also utilized SrtA-mediated transpeptidation to facilitate crosslinking of PEG-peptide hydrogels [36]. While previous work has demonstrated the utility of SrtA in hydrogel crosslinking, degradation, and ligand immobilization [36, 53, 54, 60, 61], this unique reversible enzymatic reaction has not been explored for dynamically and reversibly modulating hydrogel crosslinking density.

In this work, thiol-norbornene photoclick chemistry was used to prepare the PEG-peptide conjugates needed for investigating SrtA-induced hydrogel crosslinking (**Fig. 1**). A functional group substitution of ~70% was obtained for the PEG-GGGG conjugate. This could be a result

of peptide damage caused by extended UV irradiation and/or simply an inherent limitation in conjugation efficiency. If desired, these PEG-peptide conjugates may also be prepared using Michael-type addition between cysteine-bearing peptides and PEG-vinylsulfone or PEG-maleimide. Nevertheless, we were able to use these PEG-peptide conjugates to form hydrogels with tunable gelation time (from minutes to hours) by simply adjusting enzyme concentration in the precursor solution. A relatively high concentrations of SrtA were required for rapid crosslinking of hydrogels in this study compared with previous results [53]. While this may be caused by lower substitution (~70%) of the PEG-peptide substrate, macromer functionality (e.g., 8 in this study, compared with tens to hundreds in modified hyaluronic acid) may also be the reason of a reduced crosslinking efficiency. In addition to controlling network crosslinking, the reversible SrtA-mediated transpeptidation was also exploited to degrade PEG-peptide hydrogels, a strategy similar to that recently reported for complete gel dissolution [54]. Deferring from previous work where soluble glycine substrates were used in conjunction with SrtA, we discovered that adding SrtA alone could result in complete hydrogel degradation, albeit at a slower rate (i.e., several days) (**Fig. 2C**). During the exploration of degrading SrtA-crosslinked hydrogels, we could not obtain partially degraded hydrogels without simultaneously losing hydrogel mass. This was likely because all of the crosslinked peptide products (i.e., LPRTGGG) were substrates for SrtA (**Fig. 1A**). Gel mass loss (**Fig. 2**) was a direct result of losing PEG macromers, which occurred when all peptide products surrounding the macromer were cleaved. While this degradation method is beneficial for eroding hydrogel to recover cells or other encapsulated biologics, it is not ideal when only partial gel degradation (i.e., a loosened gel network without losing gel mass) is desired. To this end, we show that PEG-peptide hydrogels crosslinked by thiol-norbornene photopolymerization can be designed to exhibit a wide range of degradability without complete gel erosion (**Fig. 3**). These diverse degradation schemes were made possible by combining the step-growth and idealized hydrogel network structure with SrtA-sensitive and insensitive peptide linkers.

We utilized this hydrogel platform to investigate the effects of global gel softening on localized spreading of hMSCs. Our cell spreading results (**Fig. 4**) agree with that reported in the literature where soft hydrogels (>1 kPa) promoted spreading of hMSCs than stiff gels [62]. It is worth noting that while MMP-labile linkages are sensitive to local cellular activity, local MMP-mediated degradation was not sufficient to degrade the entire hydrogel. On the other hand, SrtA was added exogenously, which led to softening of the hydrogels. Furthermore, since only 40% of the peptide crosslinks contained SrtA-sensitive sequence, the gels could be softened to a desired stiffness for evaluating the effect of temporal matrix softening on hMSCs spreading.

The reversibility of SrtA-mediated transpeptidation was also leveraged to fabricate hydrogels with dynamic matrix stiffening (**Figs. 5 to 8**). Notably, we achieved this by synthesizing a simple linear peptide crosslinker flanked with sequences of the two SrtA substrates at either end of the peptide. Once crosslinked into hydrogels, the pendant SrtA substrates (i.e., LPRTG and GGG) could be covalently ligated in the presence of SrtA, creating secondary crosslinks (i.e., LPRT-GGGG) and thus increasing gel crosslinking density (**Fig. 5B** and **5C**). The stiffened gel could be subsequently softened by incubating the same gel with additional SrtA and a soluble glycine substrate (**Fig. 5D**). We experimentally determined that at least 3 hours of incubation was necessary for complete stiffening as a maximum degree of stiffening was observed at that time. Of note, an excess of oligoglycine substrate was used to drive the reaction towards complete transpeptidation [58, 63]. SrtA-mediated hydrolytic degradation can also be utilized to achieve gradual softening of the stiffened hydrogels without adding soluble glycine (**Fig. 5E**). This process was irreversible as the product LPRT-OH is not a substrate for SrtA. Furthermore, the degradation rate of hydrolysis-based gel degradation was drastically slower than transpeptidation-mediated degradation. Most importantly, multiple cycles of physiologically relevant degree of stiffening and softening could be reversibly achieved

through the same enzymatic reaction (**Fig. 6**) and without the need for using specialized macromers or potentially cytotoxic stimuli (e.g., UV light).

A pancreatic cancer cell (PCC) line COLO-357 was used in this study to illustrate the effect of dynamic matrix properties on the growth and chemo-resistance of tumor spheroids. A PCC line was chosen due to its association with a dense stroma that is scant with vasculature [1]. Here, we exposed the cell-laden hydrogels to SrtA alone to induce gel stiffening (**Figs. 5** and **6**). These additional peptide crosslinks were subsequently resolved with the use of SrtA and excess soluble glycinamide (**Fig. 6**). Cells grown in non-dynamic soft hydrogels exhibited continuous growth owing to the lower crosslinking and deformation of the network during spheroid growth (**Figs. 7B, 7C,** and **7E**). After additional crosslinking of the pendant SrtA substrates, spheroid growth was reduced and exhibited characteristics similar to that in the non-dynamic stiff gels (**Figs. 7B, 7D,** and **7E**). Of note, the density of the spheroids in the hydrogels appears to increase with stiffening, which was caused by stiffening-induced volumetric shrinkage of the hydrogel. Additional on-demand softening on day 14 'loosened' the hydrogel network, thus permitting further spheroid growth and reducing the apparent spheroid density (**Figs. 7B, 7C,** and **7E**). Here, spheroid diameter was used as a metric to evaluate the effect of dynamic hydrogel crosslinking on the growth of cancer spheroids. Our results are consistent with previous observations suggesting that proliferation of COLO-357 spheroids is affected by hydrogel crosslinking [64]. Dynamic matrix stiffening also influenced the viability and proliferation of PCCs under gemcitabine treatment (**Fig. 8**). Whereas gemcitabine induced cell death and inhibited cellular metabolic activity in both the soft and softened hydrogels, cell deaths in the non-dynamic stiff and dynamically stiffened hydrogels were limited (**Fig**. **8D**, **8E,** and **8F**). These results implied that PCCs could potentially evade drug treatment in a stiffened environment. One clinically relevant anti-PDAC therapy is to induce stromal tissue degradation while treating PCCs with chemotherapy [65]. Our results show that the majority of the cells encapsulated in the dynamically softened hydrogels remained alive following gemcitabine

treatment (**Fig. 8C**). This suggests that targeting stromal tissue by local matrix degradation may not be as effective as the cells would have been 'de-sensitized' to drug treatment after experiencing a period of stiffened matrix. More molecular characterizations are necessary to elucidate the mechanisms by which matrix mechanics regulate PCC behavior and drug sensitivity in 4D. Furthermore, studies using tumor-associated matrices (i.e., hyaluronic acid) may also improve the clinical relevance of the material design. Nonetheless, through establishing a cyclic/reversible dynamic hydrogel platform, this work has broadened the utility of SrtA-mediated transpeptidation in biomedical applications.

## 5. Conclusion

In conclusion, we have established a dynamic cell culture platform via SrtA-mediated reversible transpeptidation. The highly specific enzymatic reaction permits predictable, tunable, and reversible modulation of matrix stiffness. We identified the critical parameters for achieving on-demand hydrogel stiffening and softening. These conditions were cytocompatible for stem and cancer cells, suggesting the potential of this system in biomedical applications. We demonstrated that softened matrices permitted spreading of hMSCs, whereas reversibly stiffening matrices conferred control of cell spheroid growth. Stiffening hydrogels also promoted drug resistance behaviors and upregulated expression of SHH and ANKRD1 in PCCs. Future work will focus on exploiting SrtA-mediated reversible stiffening for studying cancer invasion and dormancy as well as stem cell differentiation under spatiotemporally regulated matrix properties.

**Acknowledgement**

**The authors thank Prof. Murray Korc for providing COLO357 cells. This work was supported in part by a National Science Foundation (NSF) Faculty Early Career Development Award (CAREER, #1452390).**

**Figure captions**

**Figure 1**. (A) Schematic of reversible SrtA-transpeptidation reaction. SrtA cleaves amide bond between threonine and glycine residues of LPRTG substrate and forms a thioacyl intermediate. Nucleophilic oligoglycine or water resolve intermediate. Note that glycine-containing product, $LPRT(G)_n$, can undergo multiple cycles of transpeptidation with additional incubation with SrtA and oligoglycine. (B) SrtA-mediated gelation of PEG-peptide hydrogels. SrtA was used to initiate crosslinking between PEG-peptide conjugates. Cysteine containing SrtA substrates (i.e., CLPRTG and GGGGC) were conjugated to PEG-NB in the presence of UV light and photoinitiator LAP. (C) Test tube tilt test to track timing of sol-gel transition using 6 wt% PEG8NB-peptide conjugates, $R_{GGGG:LPRTG}$=2). Eosin-Y (1 mM, red dye) was added for image clarity.

**Figure 2.** Effect of (A) SrtA and (B) glycinamide concentration on the transpeptidation degradation of PEG-peptide hydrogels (6 wt% PEG-peptide, $R_{GGGG:LPRTG}$=2 with 48 mM glycinamide and 50 μM SrtA for (A) and (B), respectively. (C) Effect of SrtA concentration on the hydrolytic degradation of PEG-peptide hydrogels (6 wt%, $R_{GGGG:LPRTG}$=2).

**Figure 3.** (A) Schematic of SrtA-mediated peptide cleavage. (B) Effect of alanine:glycine composition on softening of PEG8NB-A-G gels (3.0 wt% PEGNB, 25μM SrtA, & 12mM GGGGC). (C) Effect of SrtA concentration on softening of PEG8NB-A-G gels (50%A:50%G, 3.0 wt%, 12mM GGGGC). (D) Effect of initial PEG8NB concentration on softening of PEG8NB-A-G gels (50%A:50%G, 25μM SrtA, & 12mM GGGGC). (E) Effect of treatment time on softening (50%A:50%G, 3.0 wt%, 12mM, 25μM SrtA, and 12mM GGGGC).

**Figure 4.** (A) Representative confocal images of encapsulated hMSCs in statically stiff and softened hydrogels. At least three z-stacked images per gel (10 slices, 100 µm thick) were taken. (Scale: 200 µm). (B) Circularity and (C) average cell area measurements of hMSCs in the statically stiff and softened hydrogels on day 14 post-encapsulation.

**Figure 5.** (A) Schematic of SrtA-mediated reversible stiffening. (B) Effect of incubation time on stiffening of PEG-peptide hydrogels (2.5 wt% PEGNB, 25 µM SrtA). (C) Effect of SrtA concentration on stiffening of PEG-peptide hydrogels (2.5 wt% PEGNB, 4 hr incubation time). (D) Effect of glycine concentration on softening of PEG-peptide hydrogels (2.5 wt% PEGNB, 25 µM SrtA). (E) SrtA-mediated hydrolytic degradation of PEG-peptide hydrogels (2.5 wt% PEGNB, 16 hour incubation).

**Figure 6.** Cyclic stiffening and softening of PEG-peptide hydrogels (2.5 wt% PEGNB). Alternating stiffening and softening correspond to 4 hr. incubations with SrtA (25 µM) and SrtA with glycinamide (15 mM), respectively.

**Figure 7.** (A) Timeline of alternate stiffening and softening of COLO-357-laden hydrogels. Hydrogels were stiffened on day 7 and softened on day 14. Time of confocal imaging is indicated by the open arrows. All imaging was completed prior to enzyme treatments (B) Representative confocal images of encapsulated COLO-357 cells in statically soft, stiff, and reversibly stiffened hydrogels. At least three z-stacked images per gel (10 slices, 100 µm thick) were taken. (Scale: 200 µm). Histogram of spheroids diameters for (C) non-dynamic soft, (D) non-dynamic stiff, and (E) reversibly stiffened and softened hydrogels (i.e., soft-stiff-soft).

**Figure 8.** (A) Timeline of gel stiffening (at D4) and softening (at D7), as well as three-day gemcitabine treatment (D10-D13). All imaging was completed prior to enzyme or drug

treatments. (B-E) Representative live/dead images of cell-laden non-dynamic soft (B), non-dynamic stiff (C), stiffened (D), and softened (E) hydrogels with and without gemcitabine treatment. At least three z-stacked images per gel (10 slices, 100 µm thick) were taken. (Scale: 200 µm). (F) Metabolic activity of encapsulated cells pre- (at D10) and post-gemcitabine treatment (at D13). Data represent Mean ± SEM (n=3, *p<0.05, **p<0.01).

**References:**

[1] M. Schober, R. Jesenofsky, R. Faissner, C. Weidenauer, W. Hagmann, P. Michl, R.L. Heuchel, S.L. Haas, J.M. Lohr, Desmoplasia and chemoresistance in pancreatic cancer, Cancers (Basel) 6(4) (2014) 2137-54.
[2] R.G. Wells, Tissue mechanics and fibrosis, Biochim Biophys Acta 1832(7) (2013) 884-90.
[3] L. Macri-Pellizzeri, B. Pelacho, A. Sancho, O. Iglesias-Garcia, A.M. Simon-Yarza, M. Soriano-Navarro, S. Gonzalez-Granero, J.M. Garcia-Verdugo, E.M. De-Juan-Pardo, F. Prosper, Substrate stiffness and composition specifically direct differentiation of induced pluripotent stem cells, Tissue Eng Part A 21(9-10) (2015) 1633-41.
[4] F. Bordeleau, B.N. Mason, E.M. Lollis, M. Mazzola, M.R. Zanotelli, S. Somasegar, J.P. Califano, C. Montague, D.J. LaValley, J. Huynh, N. Mencia-Trinchant, Y.L. Negron Abril, D.C. Hassane, L.J. Bonassar, J.T. Butcher, R.S. Weiss, C.A. Reinhart-King, Matrix stiffening promotes a tumor vasculature phenotype, Proc Natl Acad Sci U S A 114(3) (2017) 492-497.
[5] D.T. Butcher, T. Alliston, V.M. Weaver, A tense situation: forcing tumour progression, Nat Rev Cancer 9(2) (2009) 108-22.
[6] M.W. Pickup, J.K. Mouw, V.M. Weaver, The extracellular matrix modulates the hallmarks of cancer, EMBO Rep 15(12) (2014) 1243-53.
[7] N. Gjorevski, N. Sachs, A. Manfrin, S. Giger, M.E. Bragina, P. Ordonez-Moran, H. Clevers, M.P. Lutolf, Designer matrices for intestinal stem cell and organoid culture, Nature 539(7630) (2016) 560-564.
[8] K.E. Sullivan, K.P. Quinn, K.M. Tang, I. Georgakoudi, L.D. Black, 3rd, Extracellular matrix remodeling following myocardial infarction influences the therapeutic potential of mesenchymal stem cells, Stem Cell Res Ther 5(1) (2014) 14.
[9] A.J. Rice, E. Cortes, D. Lachowski, B.C.H. Cheung, S.A. Karim, J.P. Morton, A. Del Rio Hernandez, Matrix stiffness induces epithelial-mesenchymal transition and promotes chemoresistance in pancreatic cancer cells, Oncogenesis 6(7) (2017) e352.
[10] A.V. Nguyen, K.D. Nyberg, M.B. Scott, A.M. Welsh, A.H. Nguyen, N. Wu, S.V. Hohlbauch, N.A. Geisse, E.A. Gibb, A.G. Robertson, T.R. Donahue, A.C. Rowat, Stiffness of pancreatic cancer cells is associated with increased invasive potential, Integr Biol (Camb) 8(12) (2016) 1232-1245.
[11] J.W. Shin, D.J. Mooney, Extracellular matrix stiffness causes systematic variations in proliferation and chemosensitivity in myeloid leukemias, Proc Natl Acad Sci U S A 113(43) (2016) 12126-12131.
[12] A.J. Engler, S. Sen, H.L. Sweeney, D.E. Discher, Matrix elasticity directs stem cell lineage specification, Cell 126(4) (2006) 677-89.
[13] A.M. Rosales, K.M. Mabry, E.M. Nehls, K.S. Anseth, Photoresponsive Elastic Properties of Azobenzene-Containing Poly(ethylene-glycol)-Based Hydrogels, Biomacromolecules 16(3) (2015) 798-806.
[14] A.M. Rosales, S.L. Vega, F.W. DelRio, J.A. Burdick, K.S. Anseth, Hydrogels with Reversible Mechanics to Probe Dynamic Cell Microenvironments, Angew Chem Int Ed Engl 56(40) (2017) 12132-12136.
[15] Z. Zheng, J. Hu, H. Wang, J. Huang, Y. Yu, Q. Zhang, Y. Cheng, Dynamic Softening or Stiffening a Supramolecular Hydrogel by Ultraviolet or Near-Infrared Light, ACS Appl Mater Interfaces 9(29) (2017) 24511-24517.
[16] J. Accardo, J.A. Kalow, Reversibly tuning hydrogel stiffness through photocontrolled dynamic covalent crosslinks, Chemical Science (2018).
[17] H. Shih, C.-C. Lin, Tuning stiffness of cell-laden hydrogel via host-guest interactions, Journal of Materials Chemistry B 4(29) (2016) 4969-4974.

[18] I.N. Lee, O. Dobre, D. Richards, C. Ballestrem, J.M. Curran, J.A. Hunt, S.M. Richardson, J. Swift, L.S. Wong, Photoresponsive Hydrogels with Photoswitchable Mechanical Properties Allow Time-Resolved Analysis of Cellular Responses to Matrix Stiffening, ACS Appl Mater Interfaces 10(9) (2018) 7765-7776.
[19] A.M. Rosales, C.B. Rodell, M.H. Chen, M.G. Morrow, K.S. Anseth, J.A. Burdick, Reversible Control of Network Properties in Azobenzene-Containing Hyaluronic Acid-Based Hydrogels, Bioconjug Chem 29(4) (2018) 905-913.
[20] R. Yang, H. Liang, Dynamic electro-regulation of the stiffness gradient hydrogels, RSC Advances 8(12) (2018) 6675-6679.
[21] M. Guvendiren, J.A. Burdick, Stiffening hydrogels to probe short- and long-term cellular responses to dynamic mechanics, Nat Commun 3 (2012) 792.
[22] R.S. Stowers, S.C. Allen, L.J. Suggs, Dynamic phototuning of 3D hydrogel stiffness, Proc Natl Acad Sci U S A 112(7) (2015) 1953-8.
[23] H.Y. Liu, T. Greene, T.Y. Lin, C.S. Dawes, M. Korc, C.C. Lin, Enzyme-mediated stiffening hydrogels for probing activation of pancreatic stellate cells, Acta Biomater 48 (2017) 258-269.
[24] S.R. Caliari, M. Perepelyuk, E.M. Soulas, G.Y. Lee, R.G. Wells, J.A. Burdick, Gradually softening hydrogels for modeling hepatic stellate cell behavior during fibrosis regression, Integr Biol (Camb) 8(6) (2016) 720-8.
[25] S.P. Zustiak, J.B. Leach, Hydrolytically degradable poly(ethylene glycol) hydrogel scaffolds with tunable degradation and mechanical properties, Biomacromolecules 11(5) (2010) 1348-57.
[26] A. Metters, J. Hubbell, Network formation and degradation behavior of hydrogels formed by Michael-type addition reactions, Biomacromolecules 6(1) (2005) 290-301.
[27] L. Shi, Y. Zhang, D. Ossipov, Enzymatic degradation of hyaluronan hydrogels with different capacity for in situ bio-mineralization, Biopolymers 109(2) (2018).
[28] B. Trappmann, B.M. Baker, W.J. Polacheck, C.K. Choi, J.A. Burdick, C.S. Chen, Matrix degradability controls multicellularity of 3D cell migration, Nat Commun 8(1) (2017) 371.
[29] A.M. Kloxin, A.M. Kasko, C.N. Salinas, K.S. Anseth, Photodegradable hydrogels for dynamic tuning of physical and chemical properties, Science 324(5923) (2009) 59-63.
[30] A. Ranga, M.P. Lutolf, J. Hilborn, D.A. Ossipov, Hyaluronic Acid Hydrogels Formed in Situ by Transglutaminase-Catalyzed Reaction, Biomacromolecules 17(5) (2016) 1553-60.
[31] G. Rocasalbas, A. Francesko, S. Tourino, X. Fernandez-Francos, G.M. Guebitz, T. Tzanov, Laccase-assisted formation of bioactive chitosan/gelatin hydrogel stabilized with plant polyphenols, Carbohydr Polym 92(2) (2013) 989-96.
[32] J.J. Roberts, P. Naudiyal, K.S. Lim, L.A. Poole-Warren, P.J. Martens, A comparative study of enzyme initiators for crosslinking phenol-functionalized hydrogels for cell encapsulation, Biomater Res 20 (2016) 30.
[33] O.B. Ayyub, P. Kofinas, Enzyme Induced Stiffening of Nanoparticle-Hydrogel Composites with Structural Color, ACS Nano 9(8) (2015) 8004-11.
[34] C.N. Salinas, K.S. Anseth, The enhancement of chondrogenic differentiation of human mesenchymal stem cells by enzymatically regulated RGD functionalities, Biomaterials 29(15) (2008) 2370-7.
[35] H.Y. Liu, M. Korc, C.C. Lin, Biomimetic and enzyme-responsive dynamic hydrogels for studying cell-matrix interactions in pancreatic ductal adenocarcinoma, Biomaterials 160 (2018) 24-36.
[36] M.R. Arkenberg, C.C. Lin, Orthogonal enzymatic reactions for rapid crosslinking and dynamic tuning of PEG-peptide hydrogels, Biomater Sci 5(11) (2017) 2231-2240.
[37] M.W.L. Popp, J.M. Antos, H.L. Ploegh, Site-Specific Protein Labeling via Sortase-Mediated Transpeptidation, Current protocols in protein science 56(1) (2009) 15.3. 1-15.3. 9.

[38] J.M. Antos, G.-L. Chew, C.P. Guimaraes, N.C. Yoder, G.M. Grotenbreg, M.W.-L. Popp, H.L. Ploegh, Site-specific N-and C-terminal labeling of a single polypeptide using sortases of different specificity, Journal of the American Chemical Society 131(31) (2009) 10800-10801.
[39] Q. Wu, H.L. Ploegh, M.C. Truttmann, Hepta-Mutant Staphylococcus aureus Sortase A (SrtA7m) as a Tool for in Vivo Protein Labeling in Caenorhabditis elegans, ACS chemical biology 12(3) (2017) 664-673.
[40] S.A. McConnell, B.R. Amer, J. Muroski, J. Fu, C. Chang, R.R.O. Loo, J. Loo, J. Osipiuk, H. Ton-That, R.T. Clubb, Protein Labeling via a Specific Lysine-Isopeptide Bond using the Pilin Polymerizing Sortase from Corynebacterium diphtheriae, Journal of the American Chemical Society (2018).
[41] K. Sarpong, R. Bose, Efficient sortase-mediated N-terminal labeling of TEV protease cleaved recombinant proteins, Analytical biochemistry 521 (2017) 55-58.
[42] Z. Wu, X. Cheng, H. Hong, X. Zhao, Z. Zhou, New potent and selective αvβ3 integrin ligands: Macrocyclic peptides containing RGD motif synthesized by sortase A-mediated ligation, Bioorganic & medicinal chemistry letters 27(9) (2017) 1911-1913.
[43] W. van't Hof, S.H. Maňásková, E.C. Veerman, J.G. Bolscher, Sortase-mediated backbone cyclization of proteins and peptides, Biological chemistry 396(4) (2015) 283-293.
[44] J.M. Antos, M.W.-L. Popp, R. Ernst, G.-L. Chew, E. Spooner, H.L. Ploegh, A straight path to circular proteins, Journal of Biological Chemistry (2009).
[45] J.G. Bolscher, M.J. Oudhoff, K. Nazmi, J.M. Antos, C.P. Guimaraes, E. Spooner, E.F. Haney, J.J. Garcia Vallejo, H.J. Vogel, W. van't Hof, Sortase A as a tool for high-yield histatin cyclization, The FASEB Journal 25(8) (2011) 2650-2658.
[46] Z. Wu, X. Guo, Z. Guo, Sortase A-catalyzed peptide cyclization for the synthesis of macrocyclic peptides and glycopeptides, Chemical Communications 47(32) (2011) 9218-9220.
[47] L.K. Swee, C.P. Guimaraes, S. Sehrawat, E. Spooner, M.I. Barrasa, H.L. Ploegh, Sortase-mediated modification of αDEC205 affords optimization of antigen presentation and immunization against a set of viral epitopes, Proceedings of the National Academy of Sciences 110(4) (2013) 1428-1433.
[48] S. Massa, N. Vikani, C. Betti, S. Ballet, S. Vanderhaegen, J. Steyaert, B. Descamps, C. Vanhove, A. Bunschoten, F.W. van Leeuwen, Sortase A-mediated site-specific labeling of camelid single-domain antibody-fragments: a versatile strategy for multiple molecular imaging modalities, Contrast media & molecular imaging 11(5) (2016) 328-339.
[49] S. Möhlmann, C. Mahlert, S. Greven, P. Scholz, A. Harrenga, In vitro sortagging of an antibody fab fragment: overcoming unproductive reactions of sortase with water and lysine side chains, ChemBioChem 12(11) (2011) 1774-1780.
[50] B.M. Paterson, K. Alt, C.M. Jeffery, R.I. Price, S. Jagdale, S. Rigby, C.C. Williams, K. Peter, C.E. Hagemeyer, P.S. Donnelly, Enzyme-mediated site-specific bioconjugation of metal complexes to proteins: Sortase-mediated coupling of copper-64 to a single-chain antibody, Angewandte Chemie International Edition 53(24) (2014) 6115-6119.
[51] K. Wagner, M.J. Kwakkenbos, Y.B. Claassen, K. Maijoor, M. Böhne, K.F. van der Sluijs, M.D. Witte, D.J. van Zoelen, L.A. Cornelissen, T. Beaumont, Bispecific antibody generated with sortase and click chemistry has broad antiinfluenza virus activity, Proceedings of the National Academy of Sciences 111(47) (2014) 16820-16825.
[52] X. Huang, A. Aulabaugh, W. Ding, B. Kapoor, L. Alksne, K. Tabei, G. Ellestad, Kinetic mechanism of Staphylococcus aureus sortase SrtA, Biochemistry 42(38) (2003) 11307-15.
[53] N. Broguiere, F. Formica, G. Barreto, M. Zenobi-Wong, Sortase A as a cross-linking enzyme in tissue engineering, Acta Biomater 77 (2018) 182-190.
[54] J. Valdez, C.D. Cook, C.C. Ahrens, A.J. Wang, A. Brown, M. Kumar, L. Stockdale, D. Rothenberg, K. Renggli, E. Gordon, D. Lauffenburger, F. White, L. Griffith, On-demand

dissolution of modular, synthetic extracellular matrix reveals local epithelial-stromal communication networks, Biomaterials 130 (2017) 90-103.
[55] H. Hirakawa, S. Ishikawa, T. Nagamune, Ca2+-independent sortase-A exhibits high selective protein ligation activity in the cytoplasm of Escherichia coli, Biotechnology journal 10(9) (2015) 1487-1492.
[56] M.D. Witte, T. Wu, C.P. Guimaraes, C.S. Theile, A.E. Blom, J.R. Ingram, Z. Li, L. Kundrat, S.D. Goldberg, H.L. Ploegh, Site-specific protein modification using immobilized sortase in batch and continuous-flow systems, Nature protocols 10(3) (2015) 508.
[57] B.D. Fairbanks, M.P. Schwartz, C.N. Bowman, K.S. Anseth, Photoinitiated polymerization of PEG-diacrylate with lithium phenyl-2,4,6-trimethylbenzoylphosphinate: polymerization rate and cytocompatibility, Biomaterials 30(35) (2009) 6702-7.
[58] C.P. Guimaraes, M.D. Witte, C.S. Theile, G. Bozkurt, L. Kundrat, A.E. Blom, H.L. Ploegh, Site-specific C-terminal and internal loop labeling of proteins using sortase-mediated reactions, Nat Protoc 8(9) (2013) 1787-99.
[59] L.A. Solchaga, K. Penick, J.D. Porter, V.M. Goldberg, A.I. Caplan, J.F. Welter, FGF-2 enhances the mitotic and chondrogenic potentials of human adult bone marrow-derived mesenchymal stem cells, J Cell Physiol 203(2) (2005) 398-409.
[60] E. Cambria, K. Renggli, C.C. Ahrens, C.D. Cook, C. Kroll, A.T. Krueger, B. Imperiali, L.G. Griffith, Covalent Modification of Synthetic Hydrogels with Bioactive Proteins via Sortase-Mediated Ligation, Biomacromolecules 16(8) (2015) 2316-26.
[61] E. Gau, D.M. Mate, Z. Zou, A. Oppermann, A. Töpel, F. Jakob, D. Wöll, U. Schwaneberg, A. Pich, Sortase-mediated surface functionalization of stimuli-responsive microgels, Biomacromolecules 18(9) (2017) 2789-2798.
[62] Z. Munoz, H. Shih, C.-C. Lin, Gelatin hydrogels formed by orthogonal thiol-norbornene photochemistry for cell encapsulation, Biomaterials Science 2(8) (2014) 1063-1072.
[63] C.S. Theile, M.D. Witte, A.E. Blom, L. Kundrat, H.L. Ploegh, C.P. Guimaraes, Site-specific N-terminal labeling of proteins using sortase-mediated reactions, Nat Protoc 8(9) (2013) 1800-7.
[64] H. Shih, T. Greene, M. Korc, C.C. Lin, Modular and Adaptable Tumor Niche Prepared from Visible Light Initiated Thiol-Norbornene Photopolymerization, Biomacromolecules 17(12) (2016) 3872-3882.
[65] C. Vennin, K.J. Murphy, J.P. Morton, T.R. Cox, M. Pajic, P. Timpson, Reshaping the Tumor Stroma for Treatment of Pancreatic Cancer, Gastroenterology 154(4) (2018) 820-838.

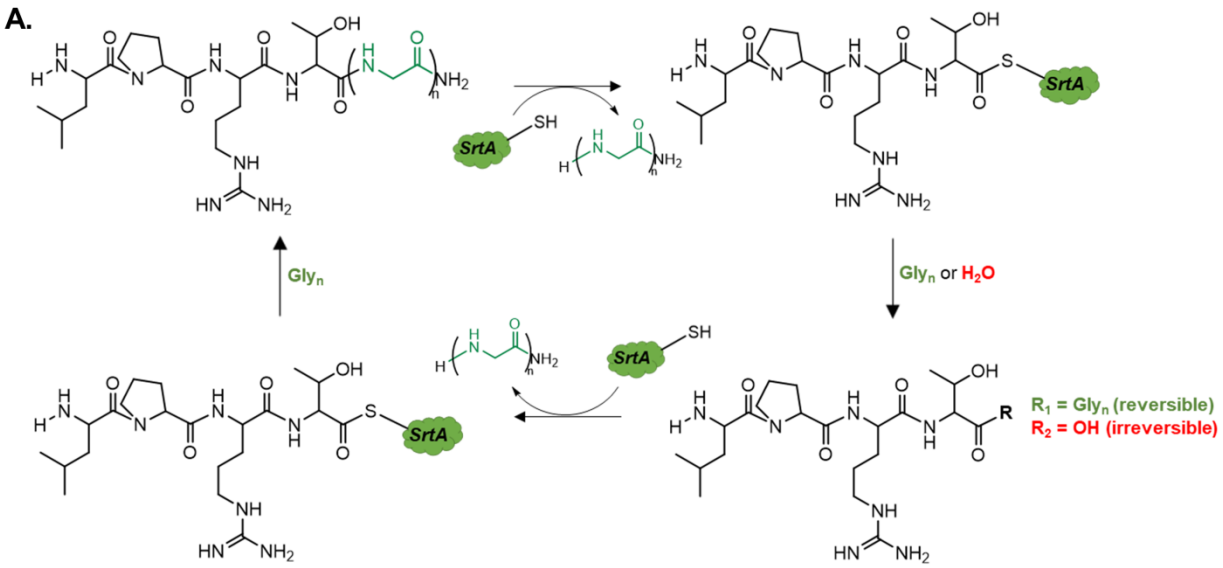
A.
SrtA
Gly$_n$
Gly$_n$ or $H_2O$
$R_1$ = Gly$_n$ (reversible)
$R_2$ = OH (irreversible)

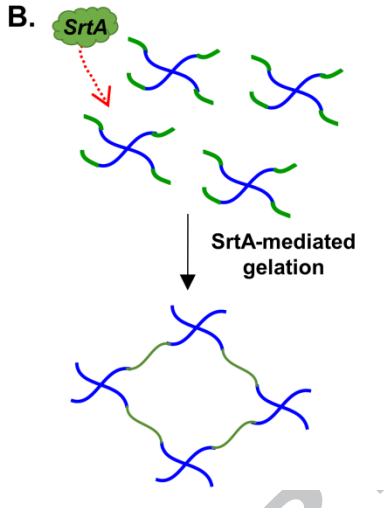
B.
SrtA
SrtA-mediated gelation

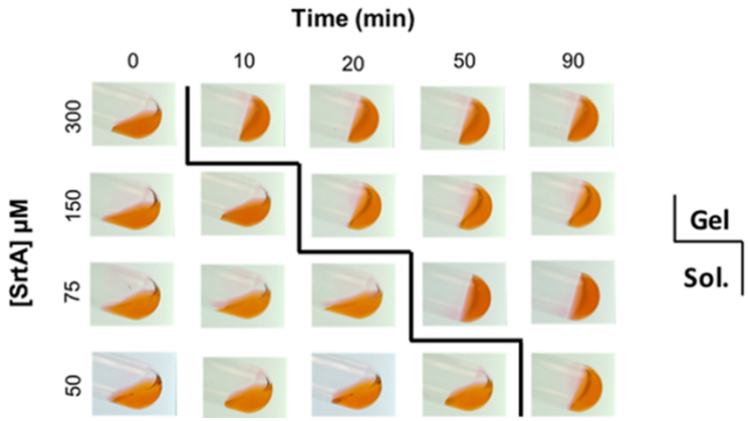
C.
Time (min)
0
10
20
50
90
[SrtA] µM
300
150
75
50
Gel
Sol.

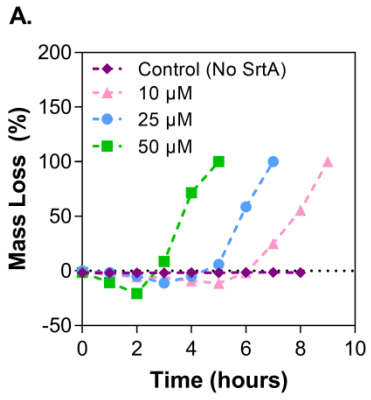
A.
Control (No SrtA)
10 µM
25 µM
50 µM
Mass Loss (%)
Time (hours)

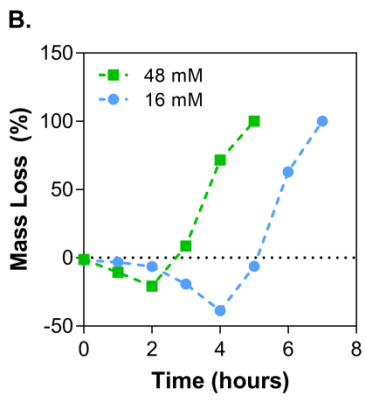
B.
48 mM
16 mM
Mass Loss (%)
Time (hours)

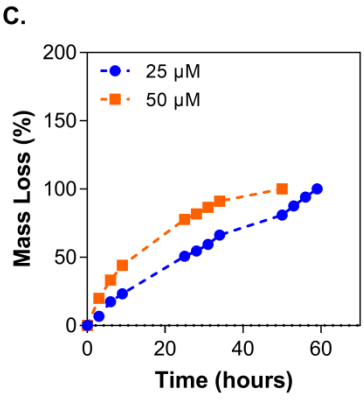
C.
25 µM
50 µM
Mass Loss (%)
Time (hours)

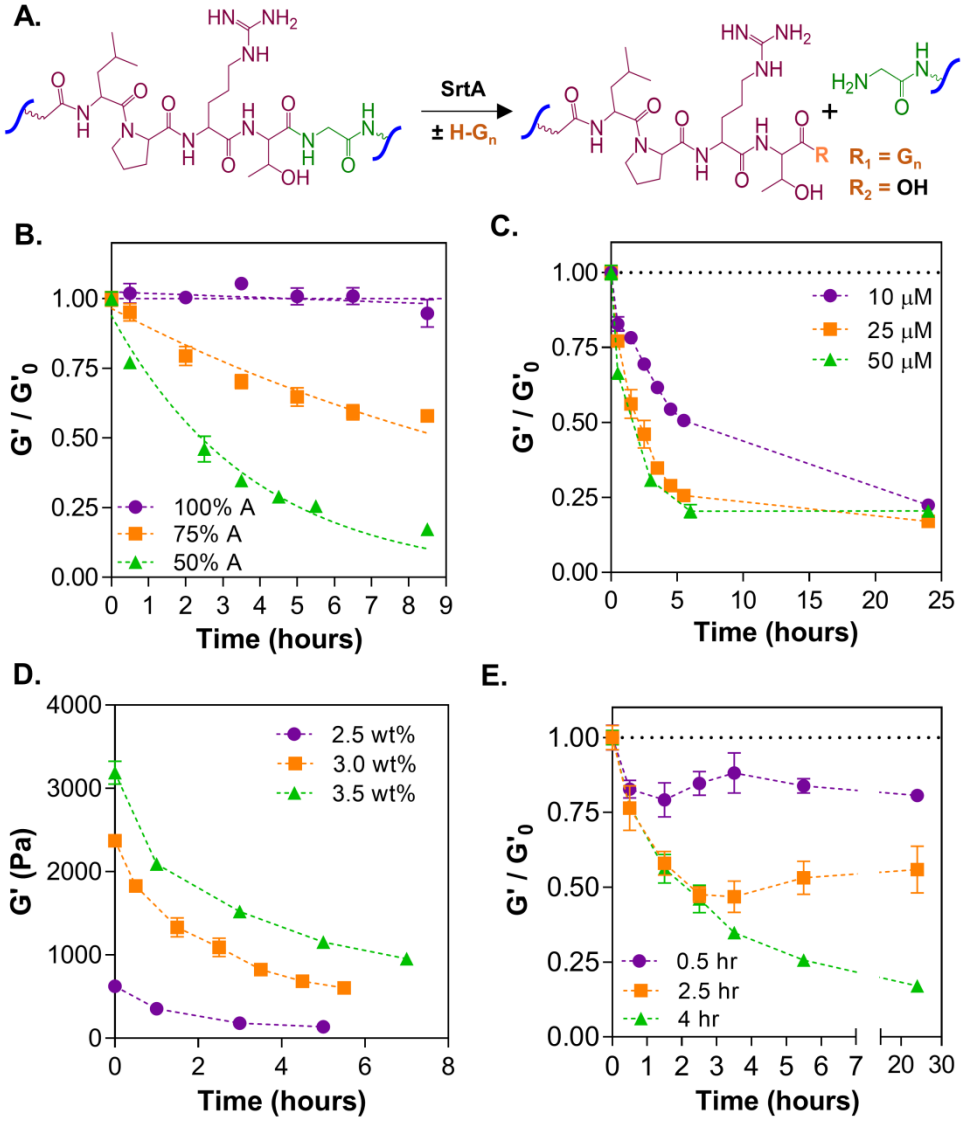

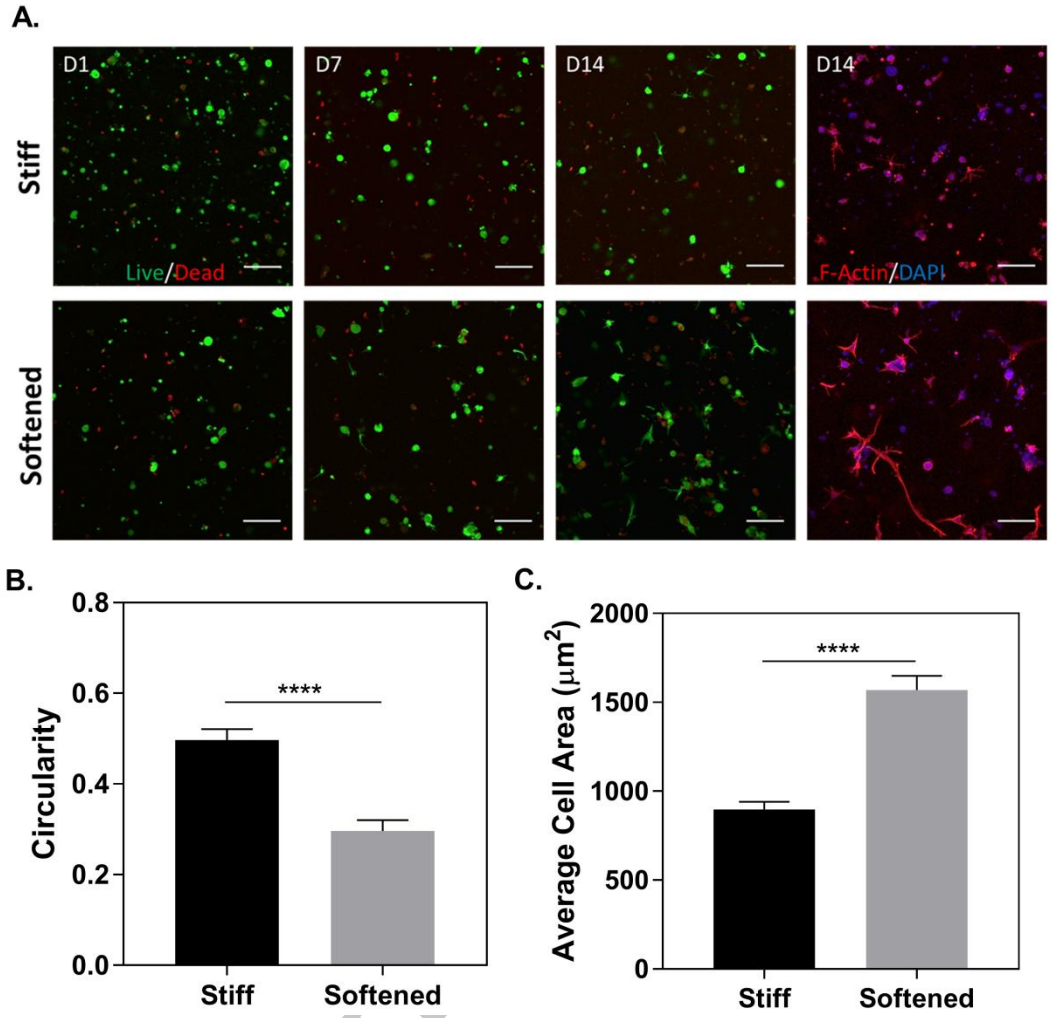

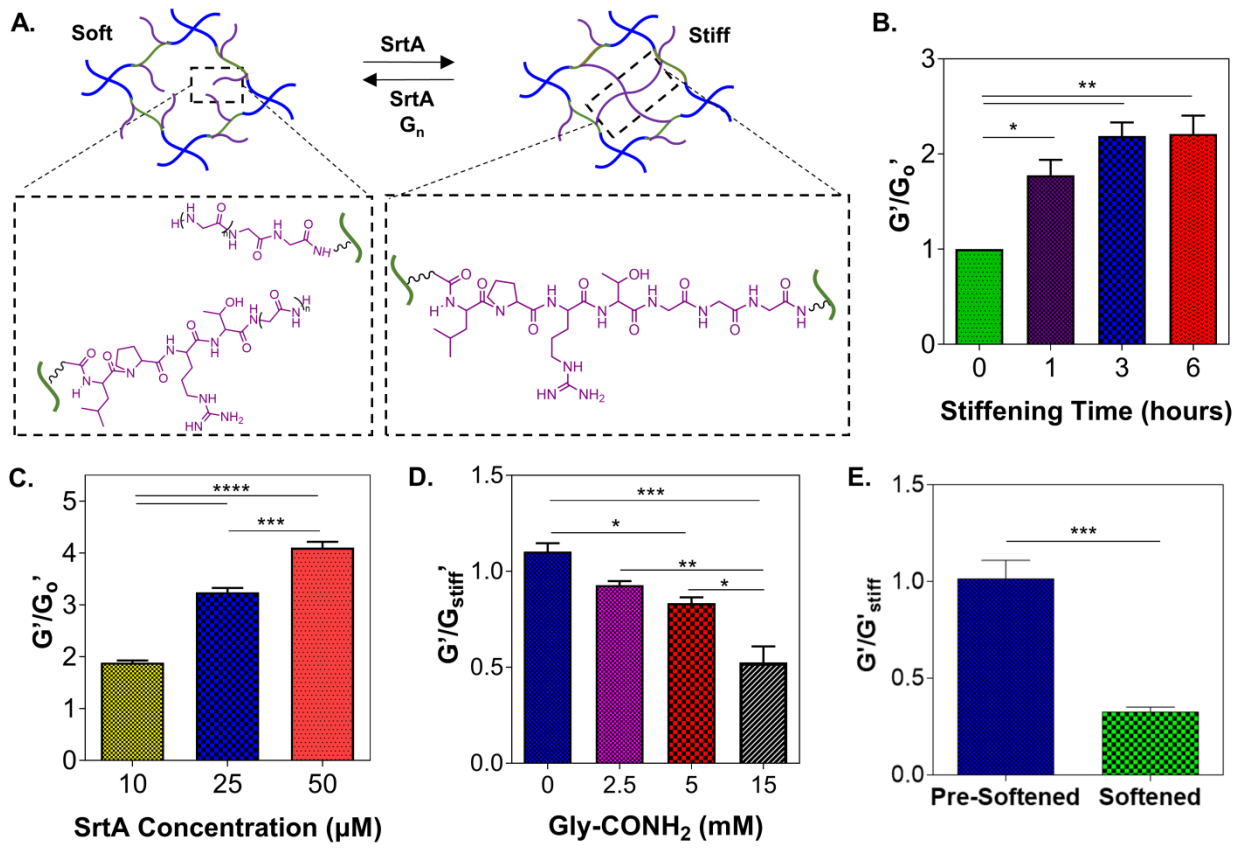
A.
Soft
SrtA
SrtA
$G_n$
Stiff
B.
$G'/G_o'$
Stiffening Time (hours)
C.
$G'/G_o'$
SrtA Concentration (μM)
D.
$G'/G_{stiff}'$
Gly-$CONH_2$ (mM)
E.
$G'/G'_{stiff}$
Pre-Softened
Softened

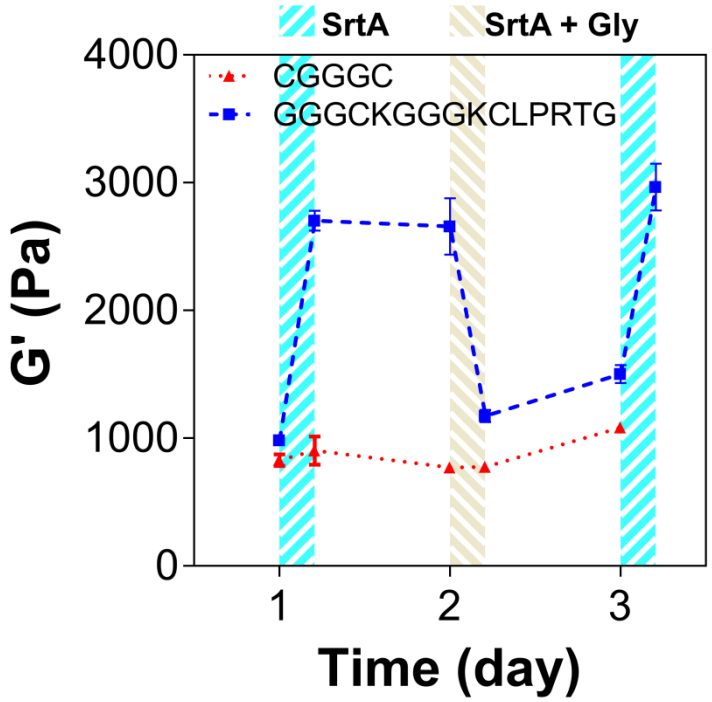
SrtA
SrtA + Gly
CGGGC
GGGCKGGGKCLPRTG
G' (Pa)
Time (day)

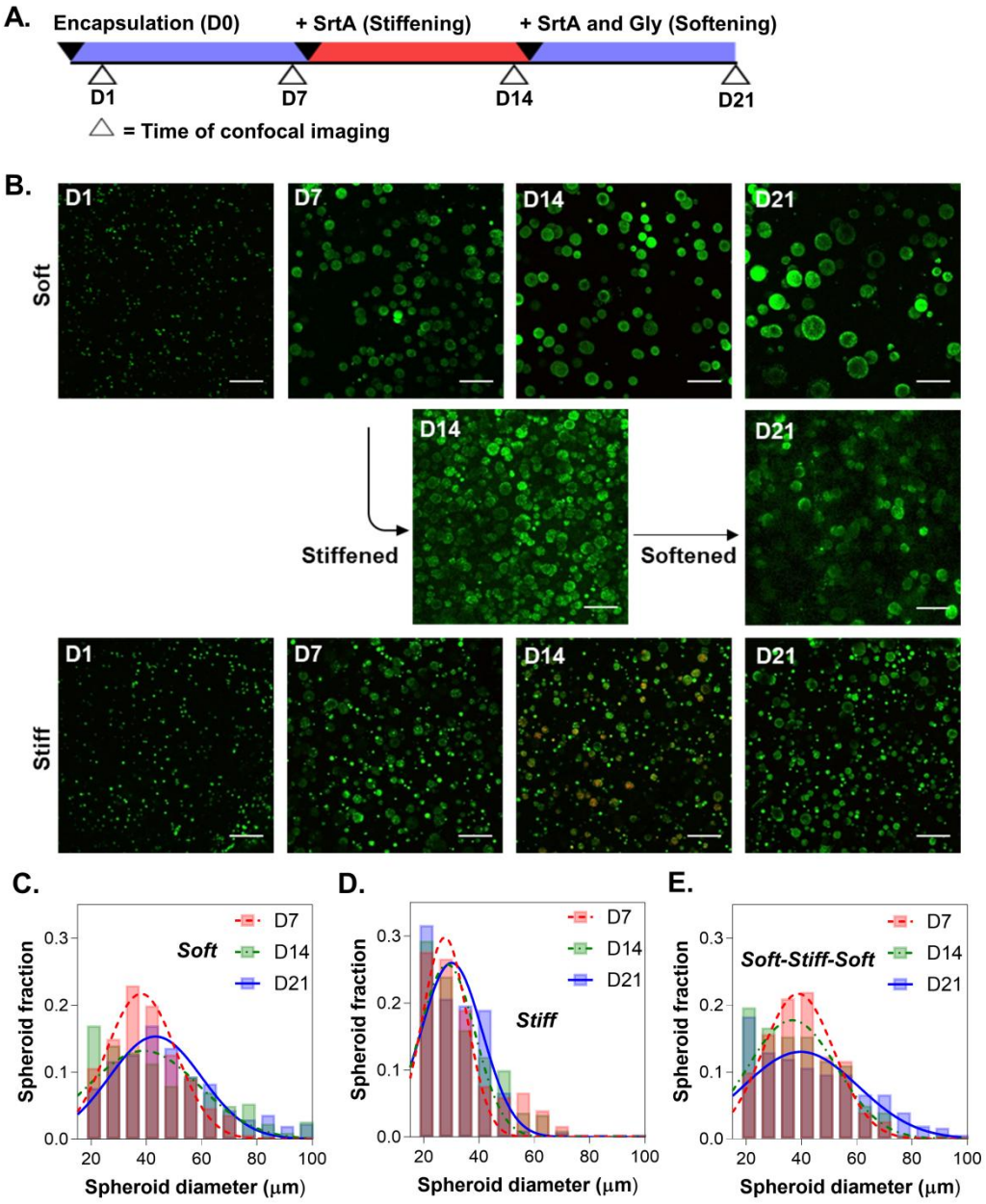

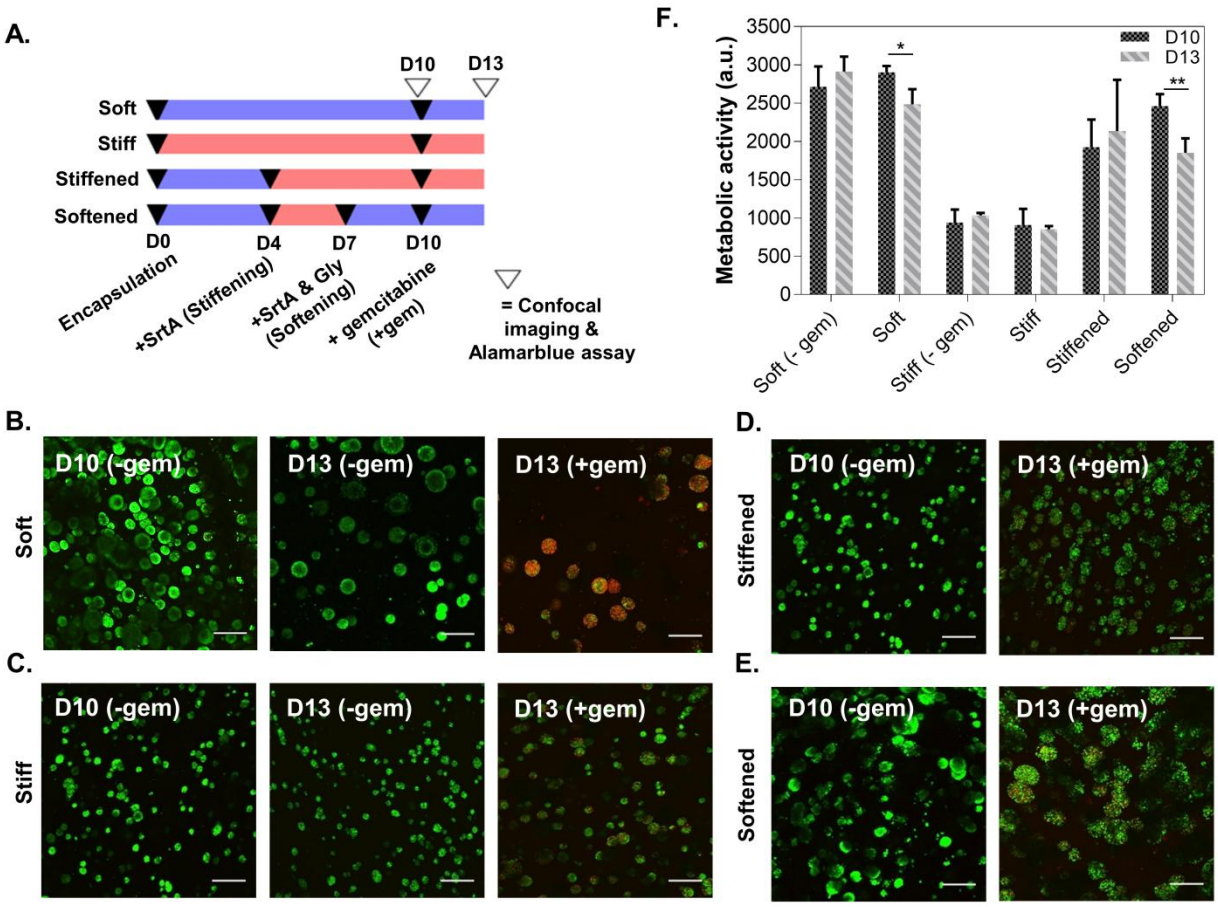


**Statement of Significance**

Cell-laden 'dynamic' hydrogels are typically designed to enable externally stimulated stiffening or softening of the hydrogel network. However, no enzymatic reaction has been used to reversibly control matrix crosslinking. The application of SrtA-mediated transpeptidation in crosslinking and post-gelation modification of biomimetic hydrogels is innovative because of the specificity of the reaction and reversible tunability of crosslinking kinetics. While SrtA has been previously used to crosslink and fully degrade hydrogels, matrix softening and reversible stiffening of cell-laden hydrogels has not been reported. By designing simple peptide substrates, this unique enzymatic reaction can be employed to form a primary network, to gradually soften hydrogels, or to reversibly stiffen hydrogels. As a result, this dynamic hydrogel platform can be

used to answer important matrix-related biological questions that are otherwise difficult to address.